Scientific Research Publishing

International Journal of Geosciences, 2023, 14, 290-303
https://www.scirp.org/journal/ijg
ISSN Online: 2156-8367
ISSN Print: 2156-8359

Methodology for Obtaining Optimal Sleeve Friction and Friction Ratio Estimates from CPT Data

Erick Baziw

Baziw Consulting Engineers, Vancouver, Canada
Email: ebaziw@bcengineers.com

How to cite this paper: Baziw, E. (2023) Methodology for Obtaining Optimal Sleeve Friction and Friction Ratio Estimates from CPT Data. *International Journal of Geosciences*, **14**, 290-303.
https://doi.org/10.4236/ijg.2023.143015

Received: January 30, 2023
Accepted: March 24, 2023
Published: March 27, 2023

Abstract

Cone penetration testing (CPT) is a cost effective and popular tool for geotechnical site characterization. CPT consists of pushing at a constant rate an electronic penetrometer into penetrable soils and recording cone bearing (q_c), sleeve friction (f_c) and dynamic pore pressure (u) with depth. The measured q_c, f_s and u values are utilized to estimate soil type and associated soil properties. A popular method to estimate soil type from CPT measurements is the Soil Behavior Type (SBT) chart. The SBT plots cone resistance vs friction ratio, R_f [where: $R_f = (f_s/q_c)100\%$]. There are distortions in the CPT measurements which can result in erroneous SBT plots. Cone bearing measurements at a specific depth are blurred or averaged due to q_c values being strongly influenced by soils within 10 to 30 cone diameters from the cone tip. The q_cHMM algorithm was developed to address the q_c blurring/averaging limitation. This paper describes the distortions which occur when obtaining sleeve friction measurements which can in association with q_c blurring result in significant errors in the calculated R_f values. This paper outlines a novel and highly effective algorithm for obtaining accurate sleeve friction and friction ratio estimates. The f_c optimal filter estimation technique is referred to as the *OSFE-IFM* algorithm. The mathematical details of the *OSFE-IFM* algorithm are outlined in this paper along with the results from a challenging test bed simulation. The test bed simulation demonstrates that the *OSFE-IFM* algorithm derives accurate estimates of sleeve friction from measured values. Optimal estimates of cone bearing and sleeve friction result in accurate R_f values and subsequent accurate estimates of soil behavior type.

Keywords

Cone Penetration Testing (CPT), Optimal Estimation, Geotechnical Site Characterization, Sleeve Friction, Cone Bearing, Friction Ratio, Iterative

Forward Modelling (IFM), Soil Behavior Type (SBT)

1. Introduction

Cone penetration testing (CPT) is a widely used and extensively researched geotechnical engineering *in-situ* test [1] [2] [3] [4] [5] for mapping soil profiles and assessing soil properties. CPT has significantly replaced the traditional methods of geotechnical site investigations such as sampling and drilling due to it being economical, repeatable, and relatively fast. The cone penetrometer has electronic sensors to measure penetration resistance at the tip and friction in the shaft (friction sleeve) during penetration. A CPT probe equipped with a pore-water pressure sensor is called a piezo-cone (CPTU cones). **Figure 1** [6] illustrates the dimensions of the most commonly utilized penetrometers. **Figure 2** [7] outlines the equations for obtaining sleeve friction and tip resistance where corrections are made for measured pore water pressures and differences in area (e.g., tip net area ratio and end area sleeve).

One of the main applications of CPT is the identification of soil type and the determination of soil stratigraphy. This soil classification facilitates grouping soils according to their engineering behavior (*i.e.*, Soil Behavior Type (SBT)) and is conventionally carried out in the laboratory where borehole samples are analyzed and classified. CPT soil classification is made by empirically relating measured q_c, f_s and u values to type of soil in SBT charts. A number of classification methods have been utilized to predict soil type from either CPT or/both

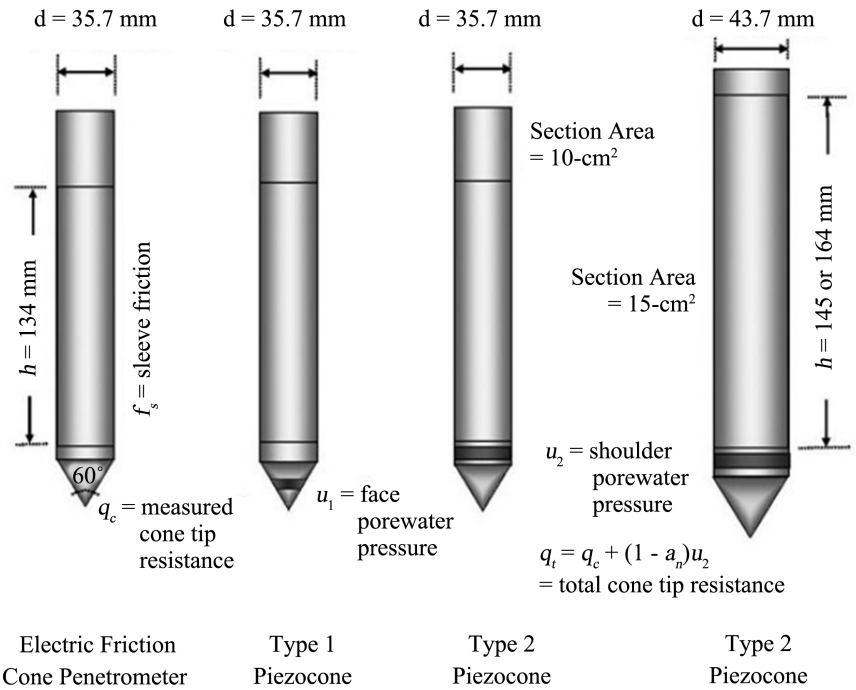

Figure 1. Standard 10 cm² and 15 cm² penetrometers [6].

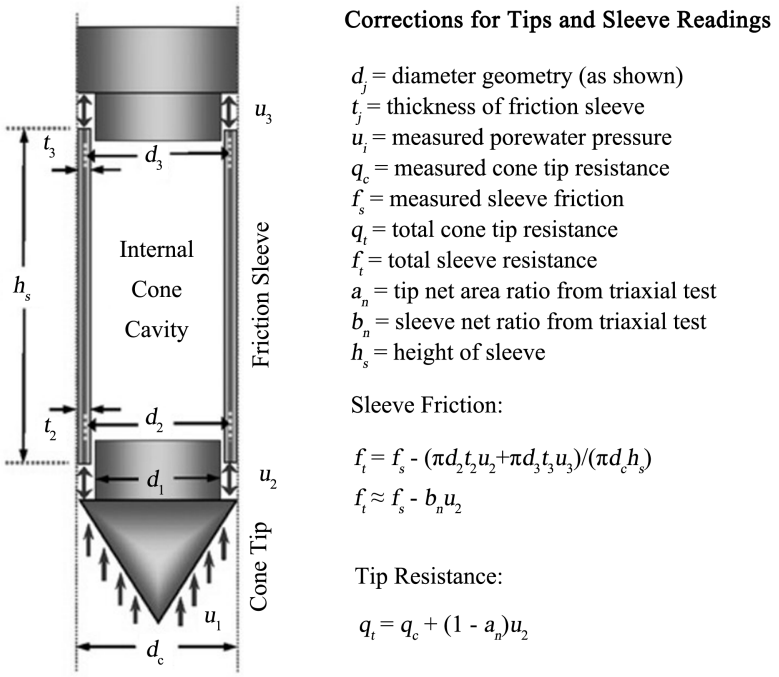

Figure 2. Determination of total cone resistance and total sleeve friction [7].

CPTu data. A very popular SBT chart was generated by Robertson *et al.* [2]. Robertson *et al.* [2] SBT chart is based on q_t and friction ratio, R_f [where: $R_f = (f_s/q_c)100\%$]. The SBT chart developed by Robertson *et al.* [2] identifies 12 soil types and is illustrated in **Figure 3**. For accurate CPT/CPTU soil classifications it is of paramount importance that cone bearing measurements of q_c and f_s with minimal distortions and added measurement errors are obtained. Unfortunately, both cone bearing and sleeve friction measurements obtain smoothed/averaged estimates of the true values.

The focus of the work outlined in this paper was to develop an optimal estimation algorithm for obtaining accurate sleeve friction and friction ratio estimates. Accurate cone bearing, sleeve friction and friction ratio estimates are of paramount importance when estimating soil behavior type from CPT date. The f_c optimal filter estimation technique (so-called *OSFE-IFM* algorithm) is subsequently outlined along with a very challenging test bed simulation. For completeness the q_c*HMM* algorithm is also subsequently summarized.

2. Mathematical Background

2.1. Cone Penetration Testing Cone Bearing Sleeve Friction Model

As previously outlined, CPT soil classifications are carried out by utilizing SBT charts where measured q_c and f_s values are empirically related to type of soil. The popular SBT chart developed by Robertson *et al.* [2] is based on q_t and friction ratio, R_f. Measured cone bearing and sleeve values are blurred/averaged. It is required to apply optimal estimation algorithms so that the effect of blurring/averaging is minimized.

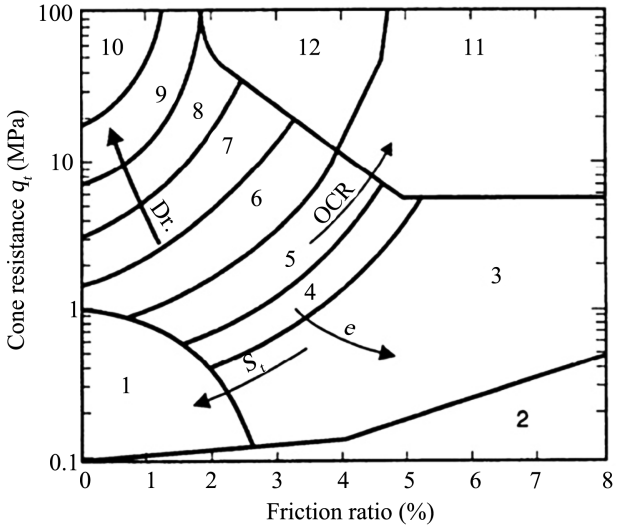

Zone	Soil Behavior Type
1	*Sensitive fine grained*
2	*Organic material*
3	*Clay*
4	*Silty Clay to clay*
5	*Calyey silt to silty clay*
6	*Sandy silt to clayey silt*
7	*Silty sand to sandy silt*
8	*Sand to silty sand*
9	*Sand*
10	*Gravelly sand to sand*
11	*Very stiff fine grained*
12	*Sand to clayey sand*

**Overconsolidated or cemented*

Figure 3. SBT chart by Robertson *et al.* [2] based on CPT cone resistance, q_t, and friction ratio, R_f (where $R_f = (f_s/q_c)100\%$).

2.2. Cone Bearing Model

The cone tip resistance measured at a particular depth is affected by the values above and below the depth of interest which results in an averaging or blurring of the true values (q_v) values [8] [9] [10] [11]. This phenomenon is especially of concern when mapping thin soil layers which is critical for liquefaction assessment. Mathematically the measured cone tip resistance q_c is described as [9] [10] [11].

$$q_c(d) = \sum_{j=1}^{60\times\left(\frac{C_d}{\Delta}\right)} w_c(j)\times q_v\left(\Delta_{qc}+j\right)+v(d)$$

$$\Delta_{qc} = \left(d-\Delta_{wc}\right), \Delta_{wc} = 30\times\left(\frac{d_c}{\Delta}\right) \quad (1)$$

where

d: the cone depth

d_c: the cone tip diameter

Δ: the q_c sampling rate

$q_c(d)$: the measured cone penetration tip resistance

$q_v(d)$: the true cone penetration tip resistance

$w_c(d)$: the $q_v(d)$ averaging function

$v(d)$: additive noise, generally taken to be white with a Gaussian pdf

In Equation (1) it assumed that w_c averages q_t over 60 cone diameters centered at the cone tip. Boulanger and DeJong [8] outline how to calculate w_c below (after correcting the equation for w_1 [9]):

$$w_c = \frac{w_1 w_2}{\sum w_1 w_2} \tag{2a}$$

$$w_1 = \frac{C_1}{1 + \left| \left(\frac{z'}{z'_{50}} \right)^{m_z} \right|} \tag{2b}$$

$$w_2 = \sqrt{\frac{2}{1 + \left(\frac{q_{t,z'}}{q_{t,z'=0}} \right)^{m_q}}} \tag{2c}$$

where

w_1: accounts for the relative influence of any soil decreasing with increasing distance from the cone tip.

w_2: adjusts the relative influence that soils away from the cone tip will have on the penetration resistance based on whether those soils are stronger or weaker.

z': the depth relative to the cone tip normalized by the cone diameter.

z'_{50}: the normalized depth relative to the cone tip where $w_1 = 0.5 C_1$.

C_1: equal to unity for points below the cone tip, and linearly reduces to a value of 0.5 for points located more than 4 cone diameters above the cone tip.

m_z: exponent that adjusts the variation of w_1 with z'.

m_q: exponent that adjusts the variation of w_2 with $\left(\frac{q_{v,z'}}{q_{v,z'=0}} \right)$.

Boulanger and DeJong [9] provide a thorough outline and review on the setting of the parameters given in Equation (2) based upon extensive research and modelling. In general terms, soils in front of the cone tip have a greater influence on penetration resistance than the soils behind the cone tip. In the subsequently outlined test bed simulations the parameters in Equation (2) are set identical to those outlined by Boulanger and DeJong. In this case, exponents $m_q = 2$ and $m_z = 3$.

Baziw and Verbeek [9] [10] [11] developed an algorithm to optimally obtain true q_v cone bearing estimates from blurred measurements q_c. The initial algorithm developed by Baziw and Verbeek [9] [10] (the so called q_c*HMM-IFM*) combined a Bayesian recursive estimation (BRE) Hidden Markov Model (HMM) filter with Iterative Forward Modelling (IFM) parameter estimation in a smoother formulation. In recent modifications and enhancements of the q_c*HMM* [11] it was possible to drop the IFM portion of the algorithm. This was predominantly accomplished by refining the HMM filter parameters.

2.3. Sleeve Friction Model

In CPT, sleeve friction is the measure of the average skin friction as the probe is advanced through the soil. Figure 4 outlines typical sleeve friction resistance and distribution generated by an algorithm (ABAQUS) which implements a Finite Element Model (FEM) designed for modelling large displacements such as those generated during CPT [12]. Figure 4(a) illustrates typical FEM sleeve friction resistance at the center of the sleeve. The high frequency fluctuations shown in Figure 4(a) are a type of measurement noise generated by the FEM algorithm due to the mesh size, the contact interface, and the parameter of soil and steel.

Figure 4(b) illustrates the FEM distribution of resistance along the length of the sleeve. In Figure 4(b) the sleeve friction close to cone tip is nearly 0 MPa and gradually increases to the uniform value of 0.029 MPa at approximately 30 mm from the bottom of the shaft for the case $\phi = 34^\circ$ and $\sigma'_{vo} = 0.05$ MPa. Susila and Hryciw [12] state that non-uniform sleeve friction distribution has been confirmed by Kiousis *et al.* [13]. Kiousis *et al.* state that there is a very thin separation between soil and cone shaft for approximately 35 mm above the upper end of the cone tip.

The sleeve friction distribution illustrated in Figure 4(b) can be thought of as a Sleeve Friction Weighting Function (SFWF) where various values of sleeve friction along the shaft (due to varying soils) are weighted to give a final measured value assumed to occur at the center of the shaft. The distribution illustrated in Figure 4(b) is mathematically approximated by Equation (3). Figure 5 illustrates the implementation of Equation (3).

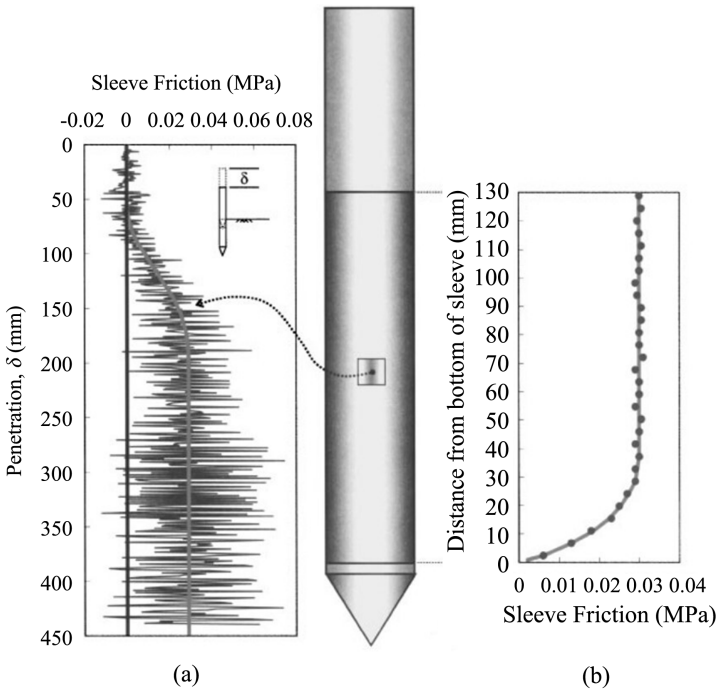

Figure 4. (a) FEM typical sleeve friction of cone sleeve during penetration. (b) FEM typical distribution of friction resistance along the sleeve ($\phi = 34^\circ$ and $\sigma'_{vo} = 0.05$ MPa) [12].

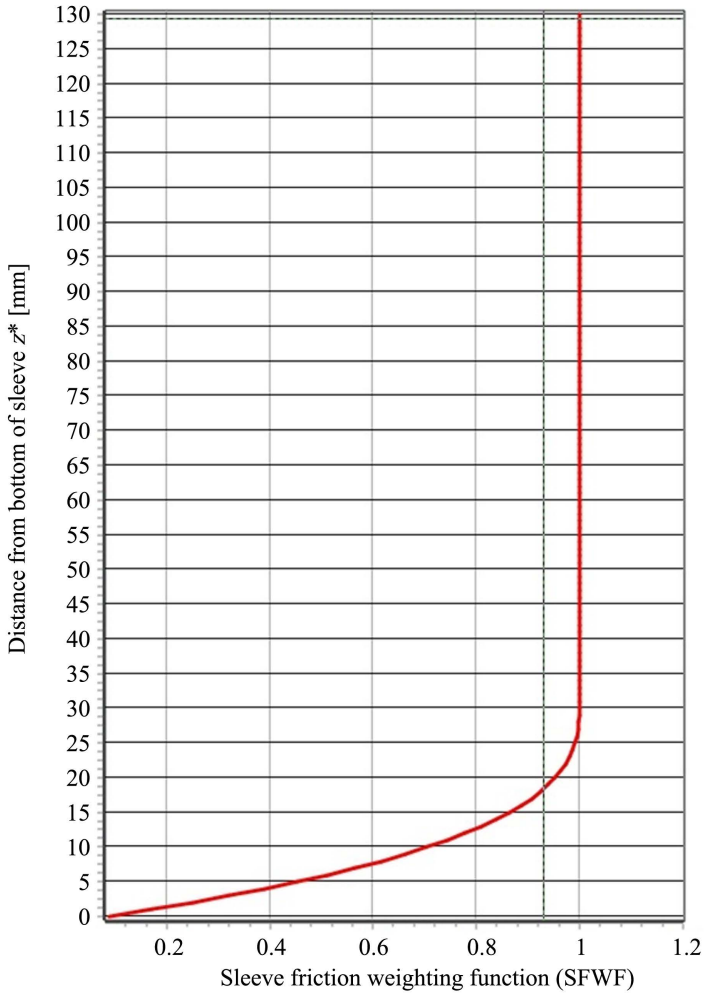

Figure 5. Mathematically modelling the sleeve distribution illustrated in **Figure 4(b)**.

$$\mathrm{SFWF}\left(z^*\right)=1 \quad \text{for } z^*>30 \text{ mm} \tag{3a}$$

$$\mathrm{SFWF}\left(z^*\right)=abs\left(z^*-30\right)^3\Big/30^3 \quad \text{for } z'\le 30 \text{ mm} \tag{3b}$$

where

z^* = the distance from bottom of sleeve

SFWF = Sleeve Friction Weighting Function

The weighting of the true sleeve friction values by the SFWF coupled with blurring of the q_v values can result in significant distortions in the calculated friction ratio R_f. **Figure 6** illustrates a simulation of cone bearing, sleeve friction and friction ratio (it assumed that both q_c and f_c have been corrected for pore pressure). In **Figure 6**, the true values of q_v, fv and R_{fv} are red traces while the corresponding measured values are the black traces. **Table 1** outlines the corresponding soil behavior types (based on the SBT chart of **Figure 3**) for the test bed simulation illustrated in **Figure 6**.

The sleeve friction measurements f_t were generated from the true sleeve friction values f_v by implementing Equation (4) outlined below.

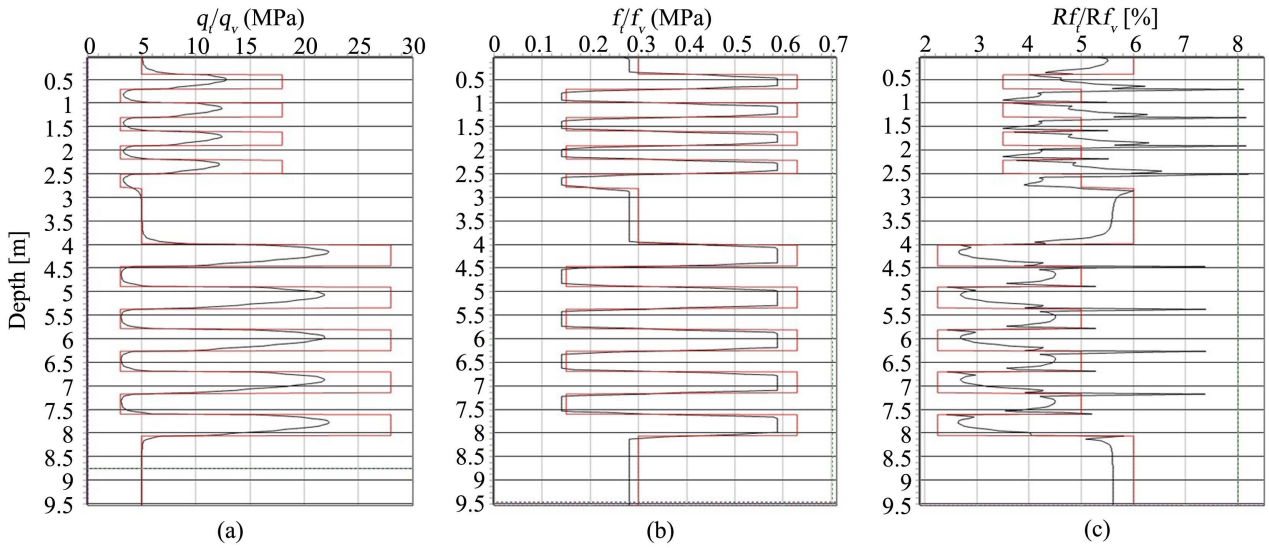

Figure 6. (a) Simulated cone bearing data q_t (measured—black trace) and q_v (true—red trace). (b) Simulated sleeve friction data f_t (measured—black trace) and f_v fv (true—red trace). (c) Simulated cone friction ratio $R_{ft} = 100 * f_t/q_t$ (measured—black trace) and $R_{fv} = 100 * f_v/q_v$ (true—red trace).

Table 1. Corresponding SBTs for test bed simulation illustrated in **Figure 6**.

q_v [MPA]	f_v [MPa]	R_{fv} [%]	Soil Behavior Type
5	0.3	6	Sand to silty sand
18	0.63	3.5	Sand
3	0.15	5	Sensitive fine grained
28	0.63	0.9	Gravely sand to sand

$$f_t(i) = \sum_{j=1}^{L^*} \mathrm{SFWF}(j) \times f_v\left(i - l^* + j\right) \tag{4}$$

where

Δ: sleeve friction sampling rate

L: sleeve friction shaft length weaker

L^*: L/Δ

l: $l/2$

l^*: l/Δ

When implementing Equation (4), Δ is initially set to a 1 mm sampling rate. The simulated date sets are then obtained by extracting data from the 1 mm sampling rate data sets at the user specified rate. This is done so that the true *in-situ* measurement conditions are simulated.

As is illustrated in **Figure 6(c)** there are significant distortions in the simulated measured friction ratios based upon the measured cone bearing and sleeve friction values. This leads to uncertainties in soil classifications. This paper outlines an optimal sleeve friction estimation algorithm. The sleeve friction optimal estimation implemented in conjunction with the q_cHMM algorithm facilitates obtaining accurate soil classification estimates.

3. *OSFE-IFM* Algorithm

The f_v optimal filter estimation technique is referred to as the *OSFE-IFM* algorithm. The *OSFE-IFM* algorithm utilizes *a posteriori* information from the q_c*HMM* algorithm and implements Iteration Forward Modelling (IFM).

3.1. *OSFE-IFM* Algorithm Formulation

The *OSFE-HMM* algorithm utilizes *a posteriori* information from the q_c*HMM* algorithm so that the solution space is reduced. The q_c*HMM* algorithm facilities quantifying the soil layering (*i.e.*, layer interfaces). This soil layering information is inputted into the *OSFE-HMM* algorithm. Soil layering can readily be quantified based upon estimated q_v values. Figure 7 illustrates Figure 6(a) where the soil layers (L_1 to L_N) are identified by blue lines and were determined from the output from the q_c*HMM* algorithm (red lines). Each of these soil layers has an associated sleeve friction values f_{v1} to f_{vN} which needs to be estimated.

The second component of the *OSFE-HMM* algorithm implements Iterative Forward Modelling (IFM) to estimate the sleeve friction values f_{v1} to f_{vN}. IFM is a parameter estimation technique which is based upon iteratively adjusting the parameters until a user specified cost function is minimized. The desired parameter estimates are defined as those which minimize the user specified cost function. The IFM technique which is utilized within the *OSFE-HMM* algorithm is the downhill simplex method (DSM) originally developed by Nelder and Mead

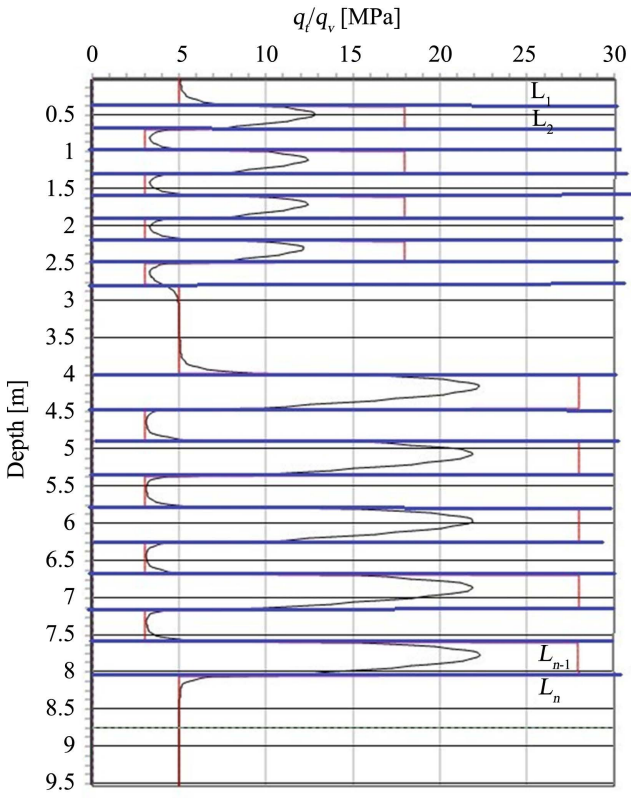

Figure 7. Illustration Figure 6(a) with estimated soil layers identified by blue lines.

[14]. The DSM in multidimensions has the important property of not requiring derivatives of function evaluations and it can minimize nonlinear-functions of more than one independent variable. A simplex defines the most elementary geometric figure of a given dimension: a line in one dimension, the triangle in two dimensions, the tetrahedron in three, etc.; therefore, in an N-dimensional space, the simplex is a geometric figure that consists of $N + 1$ fully interconnected vertices. The DSM has been used in a variety of scientific applications such as obtaining seismic source locations [15] and blind seismic deconvolution [16].

The DSM starts at $N + 1$ vertices that form the initial simplex. The initial simplex vertices are chosen so that the simplex occupies a good portion of the solution space. In addition, it is also required that a scalar cost function be specified at each vertex of the simplex. The DSM searches for the minimum of the costs function by taking a series of steps, each time moving a point in the simplex away from where the cost function is largest. The simplex moves in space by variously reflecting, expanding, contracting, or shrinking. The simplex size is continuously changed and mostly diminished, so that finally it is small enough to contain the minimum with the desired accuracy.

For the *OSFE-HMM* algorithm, the IFM cost function to be minimized is the RMS difference between the measured sleeve friction values and synthetic sleeve friction measurements generated by implementing Equation (4) with the estimated sleeve friction values f_{v1} to f_{vN} used as input. As with the test bed simulation, when implementing Equation (4) in *OSFE-HMM* algorithm, Δ is initially set to a 1 mm sampling rate. The synthetic sleeve friction measurements are then obtained by extracting data from the 1 mm sampling rate data sets at the user specified rate. This is done so that the true *in-situ* measurement conditions are replicated.

3.2. *OSFE-IFM* Test Bed Example

The performance of the *OSFE-IFM* algorithm was evaluated by processing the challenging test bed simulation illustrated in **Figure 6**. **Figure 6** illustrates a highly variable CPT profile where it assumed that both the measured q_c and f_c have been corrected for pore pressure. In **Figure 6**, the true values of q_v, f_v and R_{fv} are red traces while the corresponding measured values are the black traces.

Figure 8 illustrates the output from the q_c*HMM* algorithm. In **Figure 8**, it is shown the test bed specified true q_v values (red line), derived measured q_t values (black line) and estimated q_v' values from the *qcHMM* algorithm (blue line). As is illustrated in **Figure 8**, the estimated q_v' values are nearly identical to the true q_v values.

Figure 9 illustrates the output from the *OSFE-IFM algorithm* after processing the measured f_t sleeve values shown in **Figure 6(b)**. In **Figure 9**, it is shown the test bed specified true f_v values (red line), derived measured f_t values (black line) and estimated f_v' values from the *OSFE-IFM* algorithm (blue line). As is illustrated in **Figure 9**, the estimated f_v' values are very close to the true f_v values.

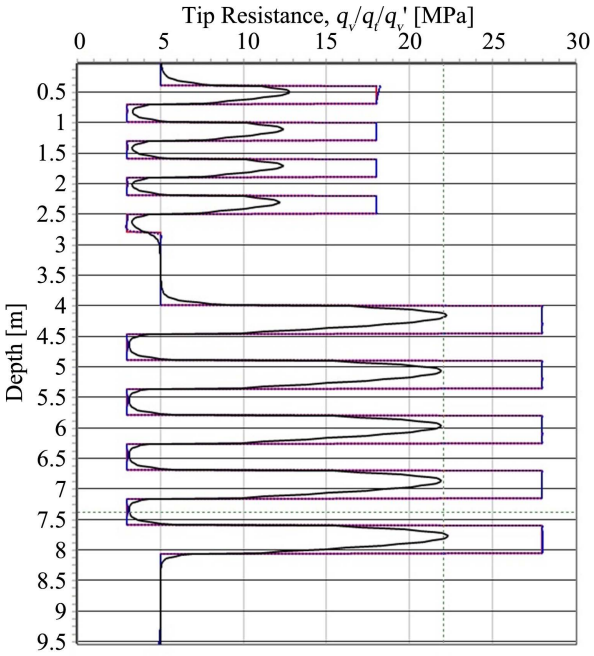

Figure 8. Specified q_v values (red line), measured q_t values (black line) and estimated q_v' values obtained from implementing the q_cHMM algorithm (blue line).

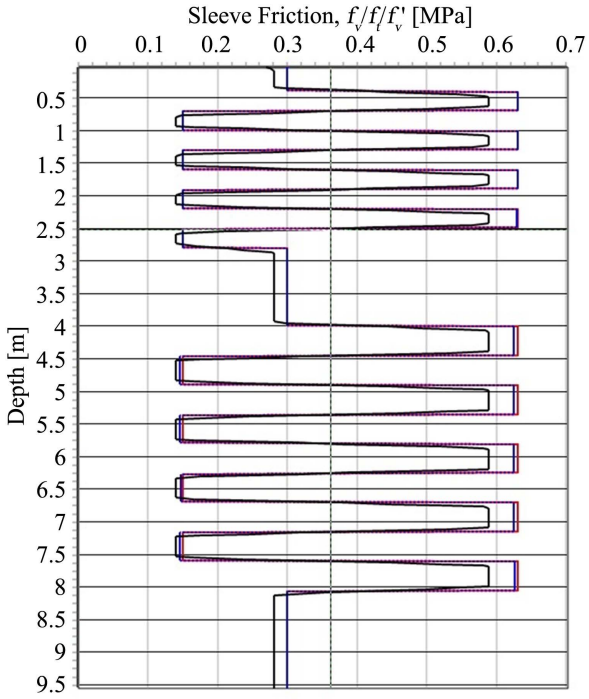

Figure 9. Specified f_v values (red line), measured f_t values (black line) and estimated f_v' values obtained from implementing the *OSFE-IFM* algorithm (blue line).

Figure 10 illustrates the friction ratio output obtained from implementation of the q_cHMM and *OSFE-IFM* algorithms where R_{fv}' values are derived from q_v' and f_v' estimates. In **Figure 10** the test bed specified R_{fv} values, measured

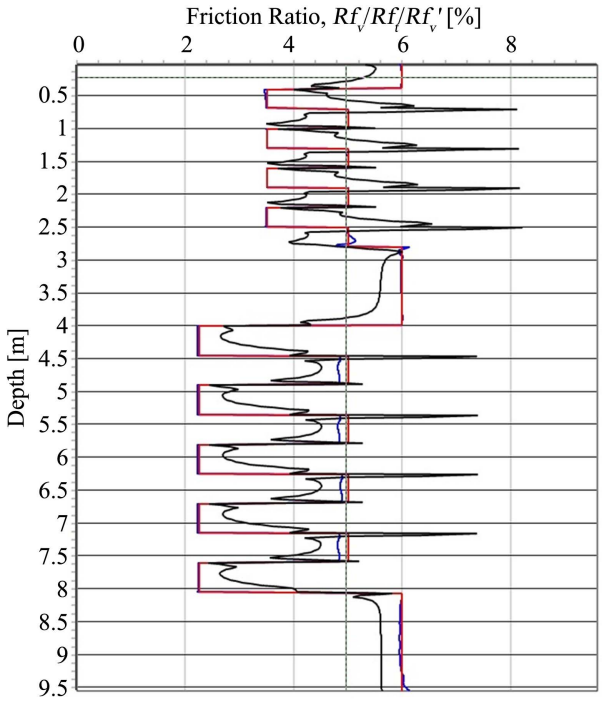

Figure 10. Specified R_{fv} values (red line), measured R_{ft} values (black line) and estimated R'_{fv} values obtained from implementing the q_cHMM and *OSFE-IFM* algorithm (blue line).

R_{ft} values and estimated R'_{fv} values are identified by red, black and blue lines, respectively. As is illustrated in **Figure 10**, the estimated R'_{fv} values are very close to the true R_{fv} values.

4. Conclusion

The cone penetration test (CPT) records cone bearing (q_c), sleeve friction (f_c) and dynamic pore pressure (u) with depth. A popular method to estimate soil type from CPT q_c, f_c and u measurements is the Soil Behavior Type (SBT) chart. The SBT plots cone resistance vs friction ratio, R_f [where: $R_f = (f_s/q_c)100\%$]. There are distortions in the CPT q_c and f_s measurements which can result in significant erroneous SBT plots. The q_cHMM algorithm was developed to address the q_c blurring/averaging. The sleeve friction measurements are also averaged along the cone sleeve shaft. This paper has outlined an algorithm (so called *OSFE-HMM* algorithm) which utilizes *a posteriori* information from the cone bearing q_cHMM estimation algorithm (*i.e.*, soil layering interfaces) and implements iteration forward modelling for obtaining optimal estimates of sleeve friction values. A challenging test bed simulation outlined in this paper has clearly shown that the *OSFE-HMM* algorithm can be implemented so that optimal sleeve friction estimates are obtained from measured values. Implementation of the q_cHMM and *OSFE-IFM* algorithms facilitates obtaining optimal friction ratio estimates. Accurate estimates of q_c, f_c and R_f are paramount for identifying soil behavior types from CPT data.

Conflicts of Interest

The author declares no conflicts of interest regarding the publication of this paper.

References

[1] Lunne, T., Robertson, P. K. and Powell, J.J.M. (1997) Cone Penetrating Testing: In Geotechnical Practice. Taylor & Francis Group, Oxfordshire.

[2] Robertson, P.K., Campanella, R.G., Gillespie, D. and Greig, J. (1986) Use of Piezometer Cone Data. *In-Situ*'86 *Use of In-Situ Testing in Geotechnical Engineering*, ASCE, Reston, 1263-1280.

[3] Robertson, P.K. (1990) Soil Classification Using the Cone Penetration Test. *Canadian Geotechnical Journal*, **27**, 151-158. https://doi.org/10.1139/t90-014

[4] ASTM D6067/D6067M-17 (2017) Standard Practice for Using the Electronic Piezocone Penetrometer Tests for Environmental Site Characterization and Estimation of Hydraulic Conductivity. ASTM Vol. 4.09, Soil and Rock (II), D5877-Latest.

[5] Cai, G.J., Liu, L.Y., Tong, L.Y. and Du, G.Y. (2006) General Factors Affecting Interpretation for the Piezocone Penetration Test (CPTU). *Journal of Engineering Geology*, **14**, 632-636.

[6] de Ruiter, J. (1971) Electric Penetrometer for Site Investigations. *Journal of the Soil Mechanics and Foundations Division*, **97**, 457-472. https://doi.org/10.1061/JSFEAQ.0001552

[7] Jamiolkowski, M., Ladd, C.C., Germaine, J.T. and Lancellotta, R. (1985) New Developments in Field and Laborator Testing of Soils. 11*th International Conference on Soil Mechanics and Foundation Engineering*, San Francisco, 12-16 August 1985, 57-154.

[8] Boulanger, R.W. and DeJong, T.J. (2018) Inverse Filtering Procedure to Correct Cone Penetration Data for Thin-Layer and Transition Effects. In: Hicks, P. and Peuchen, Eds., *Cone Penetration Testing* 2018, Delft University of Technology, The Netherlands, 25-44.

[9] Baziw, E. and Verbeek, G. (2021) Cone Bearing Estimation Utilizing a Hybrid HMM and IFM Smoother Filter Formulation. *International Journal of Geosciences*, **12**, 1040-1054. https://doi.org/10.4236/ijg.2021.1211055

[10] Baziw, E. and Verbeek, G. (2022) Identification of Thin Soil Layers Utilizing the qmHMM-IFM Algorithm on Cone Bearing Measurements. *Geo-Congress* 2022, Charlotte, 20-23 March 2022, 505-514. https://doi.org/10.1061/9780784484036

[11] Baziw, E. and Verbeek, G. (2022) Methodology for Obtaining True Cone Bearing Estimates from Blurred and Noisy Measurements. In: Gottardi, G. and Tonni, L., Eds., *Cone Penetration Testing* 2022, Baziw Consulting Engineers, Vancouver, 115-120. https://doi.org/10.1201/9781003308829-9

[12] Susila, E. and Hryciw, R.D. (2003) Large Displacement FEM Modelling of the Cone Penetration Test (CPT) in Normally Consolidated Sand. *International Journal for Numerical and Analytical Methods in Geomechanics*, **27**, 585-602. https://doi.org/10.1002/nag.287

[13] Kiousis, P.D., Voyiadjis, G.Z. and Tumay, M.T. (1988) A Large Strain Theory and Its Application in the Analysis of the Cone Penetration Mechanism. *International Journal for Numerical and Analytical Methods in Geomechanics*, **12**, 45-60. https://doi.org/10.1002/nag.1610120104

[14] Nelder, J.A. and Mead, R. (1965) A Simplex Method for Function Optimization. *Computing Journal*, **7**, 308-313. https://doi.org/10.1093/comjnl/7.4.308

[15] Baziw, E., Nedilko, B. and Weir-Jones, I. (2004) Microseismic Event Detection Kalman Filter: Derivation of the Noise Covariance Matrix and Automated First Break Determination for Accurate Source Location Estimation. *Pure and Applied Geophysics*, **161**, 303-329. https://doi.org/10.1007/s00024-003-2443-8

[16] Baziw, E. (2011) Incorporation of Iterative Forward Modeling into the Principle Phase Decomposition Algorithm for Accurate Source Wave and Reflection Series Estimation. *IEEE Transactions on Geoscience and Remote Sensing*, **49**, 650-660. https://doi.org/10.1109/TGRS.2010.2058122